

MEMS for High-Frequency Applications

Jung-Chih Chiao
Chorum Technologies,
1303 E. Arapaho Road, Richardson, TX 75081
University of Hawaii – Manoa, Honolulu, HI 96822
chiao@spectra.eng.hawaii.edu

ABSTRACT

In this paper, we reviewed some of the microelectromechanical system (MEMS) research efforts for high frequency applications. The efforts can be generally divided into two areas: planar reconfigurable transceivers and phased arrays using MEMS devices. For the planar transceivers, the interest is in demonstration of RF MEMS devices with a focus on integration issues including architectures and fabrication. Our goal is to establish building blocks for compact, smart transceivers that have beam forming and tuning functionality. For phased-array applications, system architectures were demonstrated for quasi-optical systems and phased arrays. The purpose is to demonstrate beam forming and steering functionality using MEMS devices instead of expensive phase shifters.

Keywords: Microelectromechanical system, MEMS, Millimeterwave, Antenna, Reconfigurable component, Quasi-optics

INTRODUCTION

The advantages of using millimeterwaves and submillimeterwaves have been attracting a growing interest in both academic studies and industrial applications. The urgent market demands in broadband wireless communications and high-resolution radar systems provide a strong driver and capital promise to utilize millimeterwave systems in the near future. The applications vary from commercial uses including personal communication tools [1] and automobile collision-avoidance systems [2], to scientific uses including remote sensing of the earth's surface [3] and studying emission spectra of distance celestial bodies [4]. The shorter wavelengths in the millimeterwave and submillimeterwave bands allow uses of smaller and lighter antennas and components, which makes it attractive to develop compact and portable systems, especially for air-borne and space-borne applications. The shorter wavelengths also provide broader bandwidths for communications and higher resolution for radar and imaging systems. In addition, the atmosphere attenuation of millimeterwaves is relatively low compared to infrared and optical wavelengths [5]. This allows us to build cameras and radar with ability to penetrate clouds, fog and dust for remote-sensing, missile-seeking, aircraft-guiding and automobile collision-avoidance applications.

Recent progress in monolithic millimeterwave active devices has made it possible for implementation of chip-scale integrated millimeterwave systems. High-speed transistors, which can be operated up to 300GHz, and diodes, which can be operated up to 1THz, have been routinely fabricated [6-8]. However, achievement of high-power or high-sensitivity systems is still a challenge due to the low output powers of solid-state sources and high losses in tuning and switching elements. Efforts toward reduction of insertion losses in transmission lines [9] and increase of Q-factors in inductors and filters [10,11] using micromachining techniques have shown significant improvement and great promise. To further develop complete millimeterwave systems, reconfigurable components with low losses and high Q-factors are also needed. The microelectromechanical system (MEMS) technology that utilizes micromachining techniques

to build reconfigurable devices becomes an attractive option [12,13]. MEMS devices can provide advantages of batch fabrication, fast actuation, low losses and high Qs. As frequencies increase to millimeterwaves and above, the antenna and device sizes reduce to the scales of MEMS architectures. This provides means for fast actuation with low power dissipation by microactuators[14-16]. Two- and three-dimensional reconfigurable radiation and wave-guiding structures can be constructed by using metal-coated silicon, metal-to-metal contacts and sacrificial materials on the surface of devices. This allows electromagnetic waves to propagate and be manipulated in free space and reduces dielectric losses and parasitic reactance in the substrate. The low series resistance of metal reduces insertion losses and increases Q-factors at high frequencies.

In our works, we focus our efforts in two areas: planar structures and phased arrays. For the planar structures, our interest is to demonstrate RF MEMS devices that can be integrated to make a reconfigurable transceiver. They should provide beam forming or tuning functionality and have the potential to be integrated with high-speed electronics.

For phased-array applications, we have investigated different system architectures including quasi-optical approaches and planar phased arrays. The focus is to use RF MEMS devices to replace expensive high-loss solid-state phase shifters in these systems for beam forming. Quasi-optical power combining techniques offer a promising approach to realize compact, reliable, high-power and economical systems at millimeter and submillimeter wavelengths [6,8]. A complete quasi-optical transmitter or receiver requires monolithic beam controllers for beam steering, focusing and switching. Also, in high-resolution radar applications, the phased arrays are required to generate very sharp radiation beams that can be reconfigured quickly in order to track more targets. In both systems, conventional waveguide beam-steering systems are bulky, have high losses and require expensive phase shifters. Therefore, our goal is to demonstrate means and advantages to utilize RF MEMS devices in these systems.

RECONFIGURABLE TRANSCEIVERS

We have investigated several RF MEMS components for reconfigurable transceivers. Figure 1 shows a system-level schematic drawing for such a reconfigurable transceiver. It includes a reconfigurable Vee-antenna, shunt planar backshort impedance tuners, microswitches and variable capacitors. In our architecture, flip-chip integration of monolithic millimeterwave integrated-circuits and MEMS devices is proposed. The flip-chip approach separates the fabrication of MEMS chips and electronic circuits (RF and

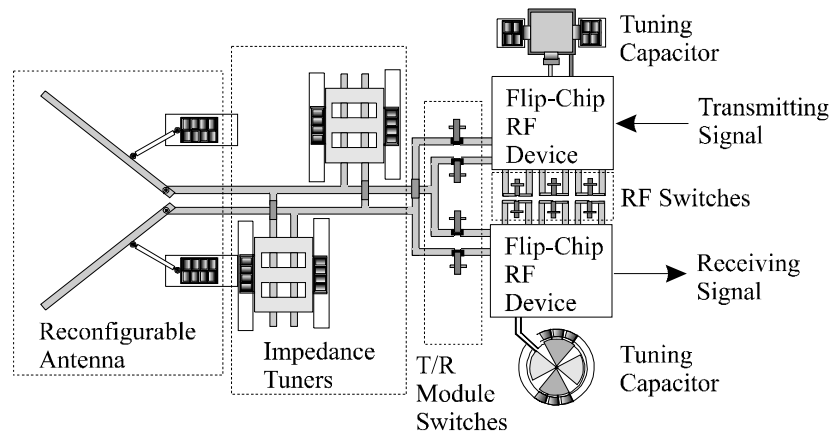


Figure 1: The architecture of a MEMS reconfigurable transceiver.

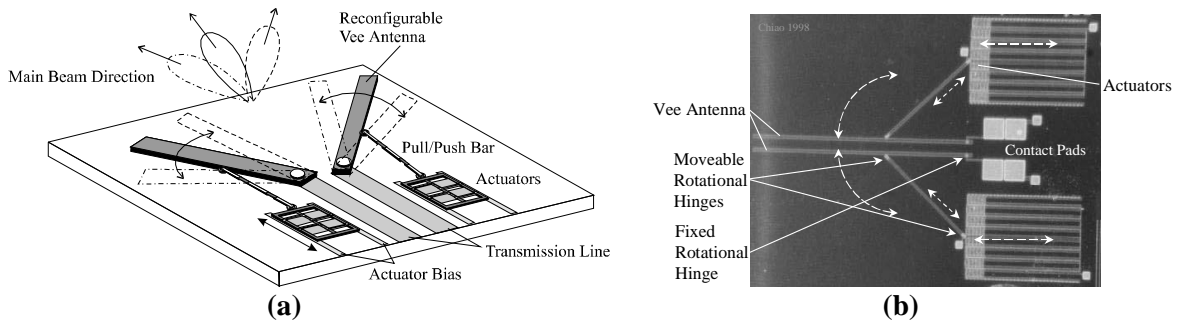


Figure 2: (a) The concept and (b) a photo of a MEMS reconfigurable Vee-antenna.

IF). It allows for integration of many different types of substrate materials, increase of yield rates and reduction of costs. The IF and low-frequency circuits can be incorporated with the MEMS devices on the same chip since the fabrication processes used for our architectures are compatible with those for CMOS circuitry.

Figure 2 shows the concept and a photo of a MEMS reconfigurable Vee-antenna. The antenna consists of two conductive arms separated with a Vee-angle. The arms are connected with pull/push bars to microactuators. The arms are moveable through pulling or pushing by microactuators. Each end of the pull/push bar has a moveable rotational hinge. The moveable rotational hinges translate the lateral motion of actuators to the circular motion of antenna arms. Each antenna arm can be controlled independently with forward- or backward-moving biases on the microactuators. When both antenna arms move in the same direction with a fixed Vee-angle, the antenna can be used to steer radiation beams. When the Vee-angle changes, radiation beam shapes can be adjusted.

The reconfigurability and antenna performance have been demonstrated for a 17.5-GHz MEMS Vee-antenna [17]. The antenna length is 1.5λ . The antenna arms were actuated to rotate (by 30° and 45°) in the same direction with a fixed Vee-angle of 75° . Figure 3 (a) shows the E-plane beam-steering and normal patterns. The peaks shift to 30° and 48° . The 3-dB beamwidths are 25° , 26° and 22° for the normal pattern, 30° - and 45° -beam-steering patterns, respectively. The beamwidths in both E- and H-planes do not change

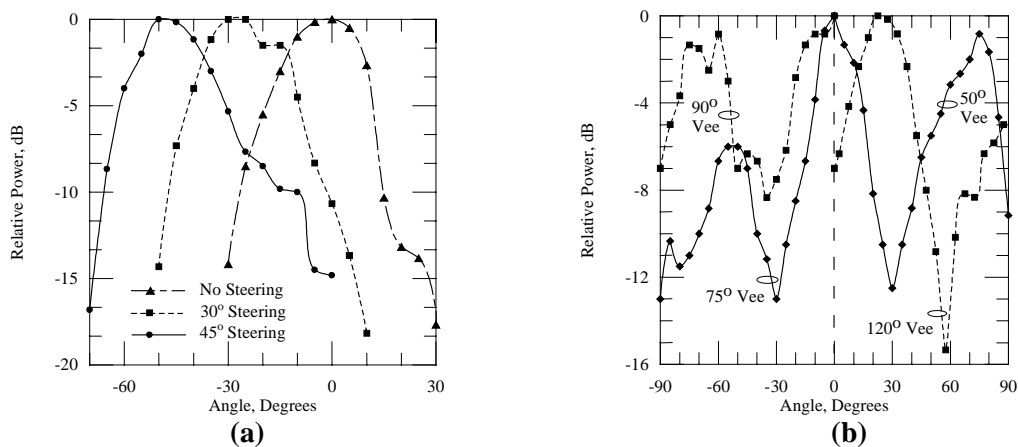


Figure 3: (a) The E-plane beam-steering patterns of a 75° Vee-antenna. (b) The co-pol normal E-plane patterns for various Vee-angles.

significantly when the antenna steers the beams. The antenna arms were actuated to rotate in the opposite directions with various Vee-angles to demonstrate the beam-shaping functionality. The co-pol E-plane patterns are shown in Fig. 3(b) with Vee-angles of 50° , 75° , 90° and 120° . Only half of the patterns are shown due to the symmetry of E-plane patterns. With a Vee-angle of 75° , a sharper main beam with lower sidelobes is obtained compared to those with Vee-angles of 50° and 90° . With a Vee-angle of 120° , a null appears in the main beam.

The architecture of the reconfigurable Vee-antennas allows monolithic integration of impedance tuners. Figure 4(a) shows a photo of a sliding planar backshort impedance tuner. The operation principle is similar to the one for mechanical waveguide backshort tuners used in metal waveguides [18]. Instead of using a moveable short-circuit load in a waveguide cavity, a sliding metal plate on top of a planar transmission line forms a moveable short-circuit. It allows a variation for the electrical length of the transmission line by varying the position of the sliding planar backshort. Therefore, a shunt transmission line with a sliding backshort plate on top can add variable shunt reactance to the load. Two shunt planar impedance tuners can perform the impedance-matching functionality. This is similar to the double-stub matching approach for microwave circuits. The planar backshort has a cascade of several low-impedance sections separated by quarter wavelengths on the sliding plate. The covered section has a lower impedance, Z_L , than the uncovered section, which has the impedance of the transmission line, Z_0 . The effective impedance of a $(2n+1)$ -section backshort plate can be approximated as $(Z_L)^{n+1}/(Z_0)^n$. The approach has been demonstrated by Lubecke [19] at 100GHz using a quasi-optical approach and a 5-section planar backshort without electrically-controlled actuators.

A planar tuner on a coplanar strips (CPS) transmission line is used for impedance tuning of antennas. The impedance tuner consists of five covered/uncovered sections, each roughly $\lambda_g/4$ long, where λ_g is the effective guided wavelength ($\lambda_g \cong 0.42\lambda_0$). The microactuators are located on the sides of sliding plate to pull the plate forward or backward. The transmission-line impedance is designed to be 50Ω and the impedance of the covered section is estimated to be 8Ω . Figure 4(b) shows the normalized magnitudes of measured and theoretical s_{21} as a function of position of the sliding plate on the transmission line. From the measured data, the maximum tuning range over a four-wavelength moving distance is 12dB. The period of the tuning curve is about $\lambda_g/2$, which agrees with the theory.

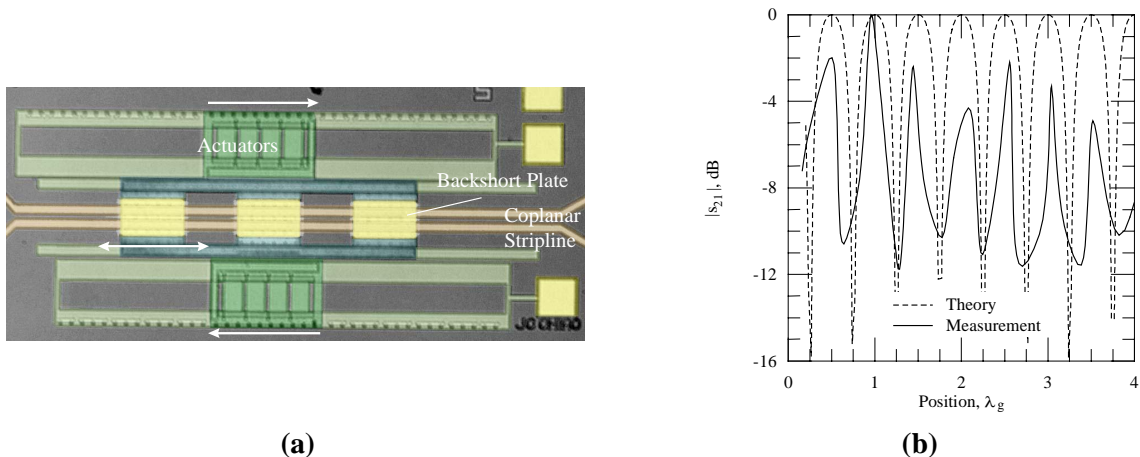


Figure 4: (a) A photo of the sliding backshort impedance tuner. (b) Measured and theoretical transmission coefficients for various positions of a 5-section impedance tuner plate on a CPS transmission line.

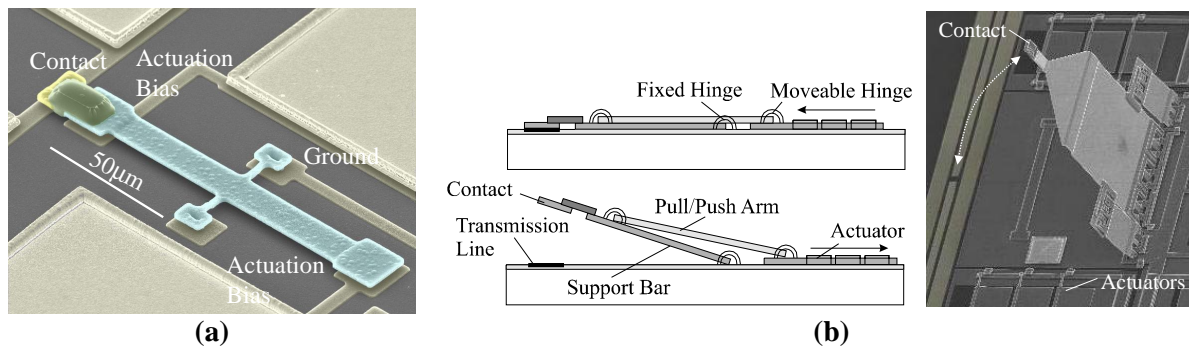


Figure 5: (a) An SEM photo of a see-saw-bar switch. (b) The concept and an SEM photo of a derrick-type switch.

Micromachining membrane-based RF switches, such as single-pole cantilever switches and air-gap switches, have been demonstrated [20, 21]. The results show low insertion losses and low power dissipation. The results are very promising and have initiated many millimeterwave applications [13]. In our approach, however, similar switches could not be integrated without changing fabrication processes used to make other MEMS devices. With a focus on integration in the proposed architectures and using the same fabrication processes, we demonstrate different MEMS switch architectures by using polysilicon and microhinges [22] to construct moveable structures.

Figure 5(a) shows an SEM photo of a see-saw-bar switch. A see-saw bar is supported by torsion posts on the sides. There are two biasing electrodes at both ends under the see-saw bar. One end of the bar is attached to a metal contact pad to make connection for an interrupted line. With actuation voltages on different biasing electrodes, the metal contact can be pulled up or pushed down by electrostatic force to open or close the connection. The air gap is about $4\mu\text{m}$ with an actuation voltage of 20V. The DC series resistance is negligible and RF performance is currently under investigation.

In a transceiver, it is required to have T/R-module switches with high RF isolation and low insertion losses. For the see-saw-bar switches, it requires a tall gap between the bar and biasing electrode. This will increase the actuation and holding voltages. To achieve high isolation and a good connection, we propose a derrick-type microswitch. Figure 5(b) shows the concept and an SEM photo of the derrick-type switch. The microactuators pull away or push forward the pull/push arms. The pull/push arms are connected to the actuators and to the sides of the support bar with moveable hinges. With one end of the support bar held by fixed hinges on the substrate, the moveable hinges on both ends of the pull/push arms translate the lateral movement of actuators to a vertical movement of the support bar. A metal contact pad, attached in the end of the support bar, will be pulled up to open, or pushed down to close the interrupted transmission line. The contact is electrically isolated from the support bar. The air gap between the contacts can be as high as $100\mu\text{m}$. This provides for the possibility of high RF isolation. The measured rising time for a $100\text{-}\mu\text{m}$ gap is $150\mu\text{s}$ and can be further reduced by shortening the pull-push arms. The strong actuation force of scratch drive actuators [16] can provide a firm contact between metal pads in order to reduce insertion losses. The measured DC resistance introduced by the contact is less than 2Ω . An isolation of 52dB was achieved at 3GHz.

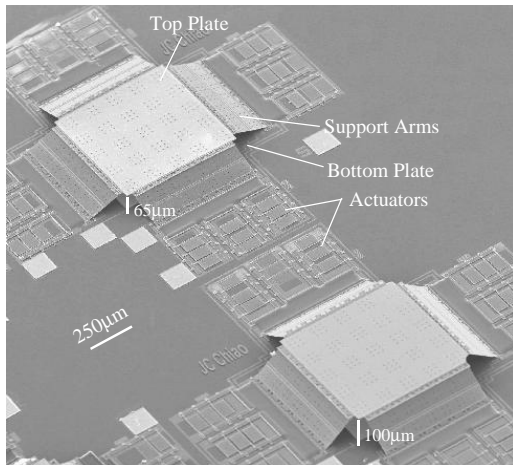


Figure 6: An SEM photo of $500\mu\text{m}\times 500\mu\text{m}$ parallel-plate variable capacitors with gap spacings of $65\mu\text{m}$ and $100\mu\text{m}$.

Different MEMS tunable capacitors have been demonstrated with goals to achieve low series resistance and high Q_s [23-25]. Figure 6 shows an SEM photo of MEMS parallel-plate variable capacitors. The variable capacitor consists of two parallel metal plates with variable gap spacing. The microactuators pull or push the support arms. The microhinges on both ends of support arms translate the lateral movement of microactuators to the vertical motion of the top metal plate in order to vary the gap spacing. The top and bottom plates are coated with gold. There are four support arms in each capacitor to actuate the top plates in order to increase the actuation force. The microactuators and capacitor structures are electrically isolated. With microactuators on both sides moving toward the plate at the same time pushing the support arms up, the gap spacing is increased. With the actuators moving away from the plate, the gap spacing is reduced. The

variable capacitance should follow the formula, $C(x) = \epsilon_0 A/x + C_p$, where the A is the plate size, x is the gap spacing, ϵ_0 is the dielectric constant of air and C_p is the parasitic capacitance. The actuators can be programmed so that not only the height of the gap is variable, but the coupling area (A) between two metal plates can also be varied for a linear operation of variable capacitance. In our design, the gap spacing can be varied between $1\mu\text{m}$ and $100\mu\text{m}$, with an increment of 20nm , giving a dynamic range of 1:100 in capacitance. Fig. 6 shows gap spacings of $65\mu\text{m}$ and $100\mu\text{m}$ in two different capacitors. Preliminary measurement shows an insertion loss less than 0.7dB from 1GHz to 50GHz . The breakdown voltages of the MEMS variable capacitors should be much higher than diode varactors. The measured breakdown voltage of a MEMS capacitor is more than 200V , where the measurement was limited by the availability of high-voltage sources.

QUASI-OPTICAL BEAM FORMERS

Quasi-optical power combining techniques combine powers in free space to eliminate dielectric losses or use of single-mode waveguides. Many solid-state high-speed devices could be incorporated through wafer-scale integration in a quasi-optical component. It is a promising approach to realize compact, reliable, higher-power and economical systems at millimeter and submillimeter wavelengths [6,26]. A complete quasi-optical transmitter or receiver requires monolithic beam-controllers for beam steering, focussing and switching. Previous efforts for quasi-optical beam-controllers considered periodic structures loaded with varactor diodes in stead of phase shifters. By controlling the biases on varactors, a linearly progressive phase shift can be provided across the aperture to steer the beam [27-29]. This approach faces the technical challenge to reduce losses caused by series resistances of Schottky diodes at high frequencies.

The idea of using reconfigurable passive elements with MEMS RF switches to provide phase shifts, instead of using varactor diodes, to reduce insertion losses has been demonstrated [30-31]. Extending the same approach to large-aperture antenna applications provides more functionality to produce multiple beams for simultaneous targeting; and dynamic reconfigurability of beam forming/switching/steering for multiple feed networks. We have demonstrated a new architecture using unit blocks to construct large-aperture arrays [32]. Figure7(a) shows the concept. The incident waves enter the grid from the right side and re-radiate from the left surface into the free space. The grid consists of 5×5 unit blocks, in which each

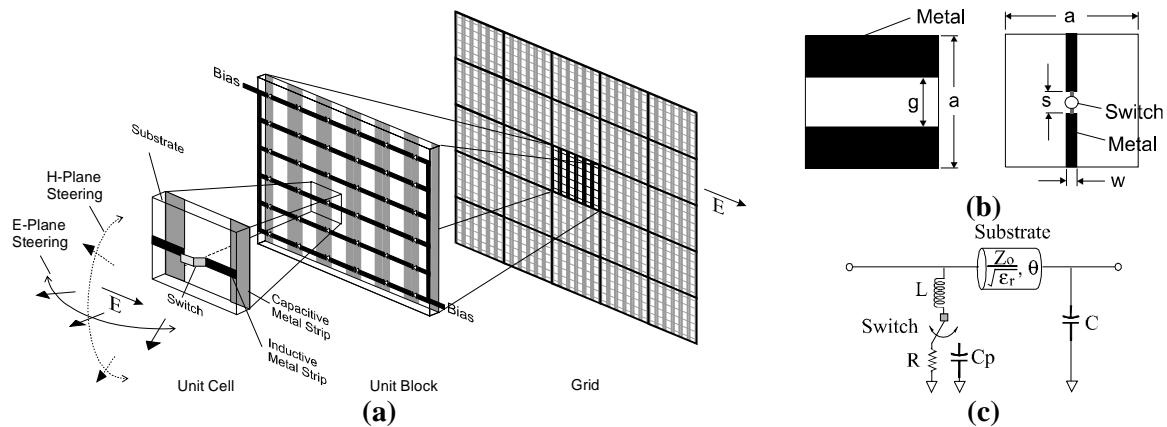


Figure 7: (a) A 900-element reconfigurable transmission-type beamformer. The 30x30 array is divided into 5x5 unit blocks. Each contains 6x6 unit cells. (b) The back and front metal patterns of a unit-cell. (c) The equivalent circuit of a unit-cell.

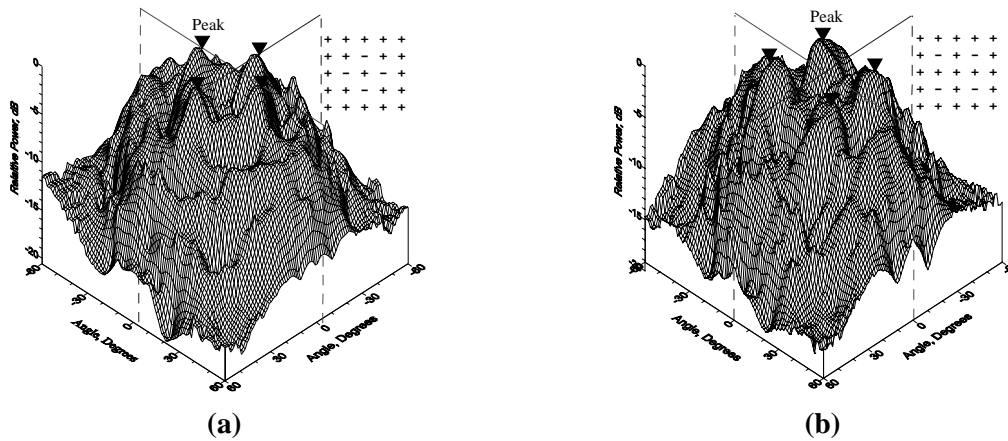


Figure 8: Multiple-beam beam forming and switching. The legends show the unit-block configurations in the array (“-”: capacitive and “+”: inductive).

block provides either a capacitive phase shift or an inductive phase shift uniformly across the unit block. Each block has 6x6 unit cells. Each unit cell has capacitive metal patterns on the back and inductive strip on the front, as shown in Fig. 7(b). The inductive strips are interrupted by switches in series. The switches change the shunt reactances for the propagation waves from inductive, when the switches are closed, to capacitive, when the switches are open. Fig. 7(c) shows the equivalent circuit. By changing the settings of switches in different unit blocks to reach different reactances, binary phase-shifts across the aperture can be achieved. A phase variation across the transmitting aperture sets the directions or shapes of the beams in the far field. The unit-block approach reduces the phase coupling between elements that have different metal patterns and simplifies control circuits.

The 5x5-block grid was reconfigured to demonstrate, using conductive tape to imitate MEMS switches, 4-way beam forming at 5GHz. The grid was rotated every 10° about the center of grid to measure the pattern in each cut-plane in order to construct 3-D patterns. Fig. 8 shows the 3-D beam patterns and the legends show the configurations of the 5x5 unit blocks. The peaks appear at ±18° and ±20° in the E- and H-planes, respectively (Fig. 8(a)). When the configuration of the grid switches to the one in Fig 8(b), the

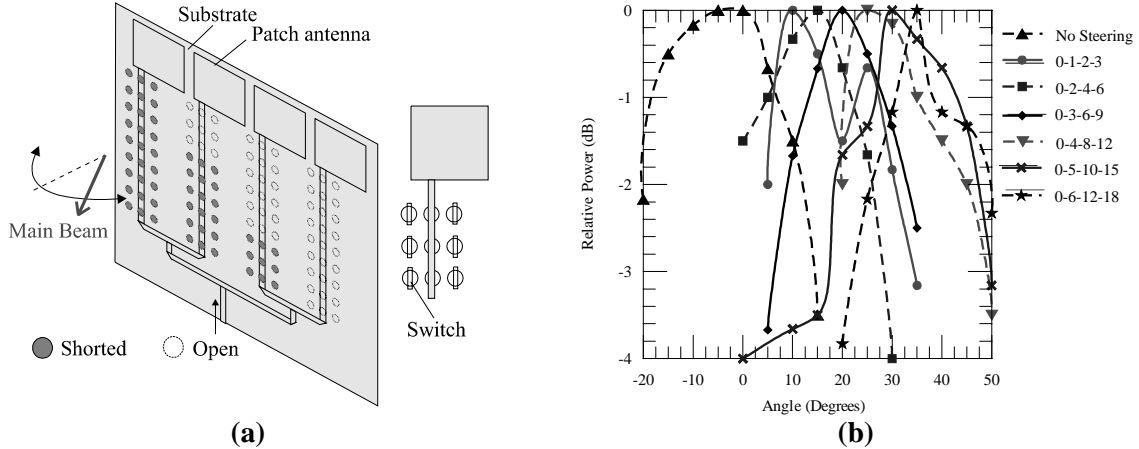


Figure 9: (a) The 4-element patch-antenna array with the reconfigurable PBG holes on the ground plane. (b) Measured patterns for the different ground-plane configurations. Full patterns from -90° to $+90^\circ$ were measured. The legends show the PBG periods (with open switches) for each antenna.

four peaks appear at $\pm 18^\circ$ in the two 45° -cutplanes. This demonstrated the functionality of forming multiple beams and beam switching. The 5-GHz model is a proof-of-concept demonstration. For millimeterwave applications, the MEMS switch arrays and metal patterns would be monolithically fabricated on wafers.

PHASED-ARRAY BEAM STEERERS

Phased-array antennas are used to steer radiation beams electronically. The applications usually need many antennas in an array in order to generate sharp beams with large scanning angles. This requires many expensive phase shifters and the number of phase shifters scales with the number of antennas in an array. In addition, an electronic phase shifter along the transmission line may be a limiting factor as to the power handling capability and nonlinearity of the antenna. In this work, we demonstrated the feasibility of using reconfigurable photonic band gaps (PBG) on ground plane with MEMS switches in order to eliminate phase shifters [33].

Photonic bandgap (PBG) ground planes in a microstrip line are periodic etched holes in the ground-plane metal. They change the propagation constant (β) in its passband [34]. At the edge of the passband, the value of β is almost double that of a normal microstrip line. This provides the possibility of phase shifting without using electronic phase shifters. Fig. 9(a) shows the architecture of phased-array antennas using MEMS RF switches to reconfigure the PBG periods in the ground plane. A four-element patch-antenna array was designed operating at 5.6GHz to demonstrate the principle. The $50\text{-}\Omega$ microstrip line feeds the patch antenna, with three columns of 18 PBG periods per column etched on the ground plane. The PBG periods can be dynamically varied using RF switches. The discrete beam-steering patterns are obtained by covering a varying number of PBG periods with conductive tape to imitate MEMS switches. The maximum phase lag between adjacent antennas is obtained when the PBG periods are configured as 0, 6, 12 and 18 (0-6-12-18) periods under the four lines, respectively. Fig. 9(b) shows the beam steering results. The different patterns have individually been normalized, nonetheless the relative peak powers of the different steering patterns varied by less than 2 dB. The beam-steering angle varies linearly as the number of PBG periods is varied and a maximum beam steering of 35° is obtained. Larger scanning

angles can be achieved by increasing the numbers of PBG periods in the ground plane and higher resolution can be achieved by increasing the number of antennas or change of array configurations.

CONCLUSIONS

In this paper, we reviewed some of the RF MEMS research efforts in the University of Hawaii. We have investigated several RF MEMS devices with a goal to build dynamically-reconfigurable transceivers for millimeterwave applications. We have also examined several system architectures for applications of RF MEMS switches. MEMS technology has launched a revolutionary approach to realize high-frequency systems and applications. Initial demonstrations show some of the advantages and potentials. However, there are still many issues to be studied such as materials, structures, packaging, RF coupling, and reliability.

ACKNOWLEDGMENTS

We appreciate the support from the HRL Laboratories and the Army Research Office.

REFERENCES

- [1] R. Leyshon, "Millimeter Technology Gets a New Lease on Life," *Microwave Journal*, No.3, pp.26-35, March 1992.
- [2] G.R. Huguenin, "Millimeter Wave Radar for Automobile Crash Avoidance Systems," *Proceedings of the International Conference on Millimeter and Submillimeter Waves and Applications*, SPIE Proceedings Series, Vol. 2250, Jan. 1994.
- [3] J.W. Waters and P.H. Siegel, "Applications of Millimeter and Submillimeter Technology to Earth's Upper Atmosphere: Results To Date and Potential for the Future," *Proceedings of the 4th International Symposium on Space Terahertz Technology*, Los Angeles, CA, March 1993.
- [4] T. Phillips, "Developments in Submillimeterwave Astronomy," *Proceedings of the 19th International Conference on Infrared and Millimeter Waves*, Sendai, Japan, 1994.
- [5] J.C. Wiltse, "Introduction and Overview of Millimeter Waves," *Infrared and Millimeter Waves*, Vol.4, Chap.1, K.J. Button, Ed., Academic Press, Inc., New York, 1979.
- [6] R.A. York, "Quasi-Optical Power Combining Techniques," *Millimeter and Microwave Engineering for Communications and Radar*, J.C. Wiltse, Ed., Critical Reviews of Optical Science and Technology, Vol. CR54, pp.63-97, 1994.
- [7] R. Zimmermann, T. Rose and T. Crowe, "An All Solid-State 1THz Radiometer for Space Applications," *Proceedings of the 6th International Symposium on Space Terahertz Technology*, Pasadena, CA, March 1995.
- [8] "THz Grid Frequency Doublers," J.-C. Chiao, A. Markelz, Y. Li, J. Hacker, T. Crowe, J. Allen and D. Rutledge, *Proceedings of the 6th International Symposium on Space Terahertz Technology*, Pasadena, CA, March 1995.
- [9] K. Herrick, T. Schwarz and L. Katehi, "Si-Micromachined Coplanar Waveguides for Use in High-Frequency Circuits," *IEEE Trans. Microwave Theory and Tech.*, Vol.46, No.6, pp.762, 1998.
- [10] C. Chi and G. Rebeiz, "Planar Microwave and Millimeter-wave Lumped Elements and Coupled-Line Filters Using Micro-Machining Techniques," *IEEE Trans. Microwave Theory and Tech.*, No.4, pp.730, 1995.
- [11] S. Robertson, L. Katehi and G. Rebeiz, "Micromachined W-Band Filters," *IEEE Trans. Microwave Theory and Tech.*, No.4, pp.598, 1996.
- [12] C. Nguyen, L. Katehi and G. Rebeiz, "Micromachined Devices for Wireless Communications," *Proc. IEEE*, Vol.86, No.8, 1998.

- [13] E. Brown, "RF-MEMS Switches for Reconfigurable Integrated Circuit," *IEEE Trans. Microwave Theory Tech.*, Vol.46, No.11, pp.1868, 1998.
- [14] L. Fan, Y.-C. Tai, R. Muller, "Integrated Moveable Micromechanical Structures for Sensors and Actuators," *IEEE Trans. of Electron Devices*, Vol.35, No.6, 1988.
- [15] W.Tang, T.Nguyen and R.Howe, "Laterally Driven Polysilicon Resonant Microstructures," *Sensors and Actuators*, Vol. 20, pp.25, Nov. 1989.
- [16] T. Akiyama, D. Collard and H. Fujita, "Scratch Drive Actuator with Mechanical Links for Self-Assembly of Three Dimensional MEMS," *J. MEMS*, Vol.6, No.1, pp.10, 1997.
- [17] J.-C. Chiao, Y. Fu, I. Chio, M. DeLisio and L. Lin, "MEMS Reconfigurable Vee Antenna," *Digest of the 1999 IEEE MTT Intl. Microwave Symposium*, Anaheim, June 1999.
- [18] W. McGrath, T. Weller and L. Katehi, "A Novel Noncontacting Waveguide Backshort for Submillimeterwave Frequencies," *J. of IR & MM*, Vol.16, No.1, pp. 237, 1995.
- [19] V. Lubecke, W. McGrath and D. Rutledge, "A 100GHz Coplanar Strip Circuit Tuned with a Sliding Planar Backshorts," *IEEE Microwave and Guided Wave Letters*, Vol.3, No.12, pp.441, 1993.
- [20] J. J. Yao and M. Chang, "A Surface Micromachined Miniature Switch for Telecommunications with Signal Frequencies from DC to 4GHz," *The 8th International Conference for Solid State Sensors and Actuators*, pp. 384, Sweden, June 25, 1995.
- [21] C. Goldsmith, J. Randall, S. Eshelman, T. H. Lin, D. Denniston, S. Chen, and B. Norvell, "Characteristics of Micromachined Switches at Microwave Frequencies," *Digest of IEEE MTT-S Symposium*, pp.1141, 1995.
- [22] K. Pister, M. Judy, S. Burgett and R. Fearing, "Microfabricated Hinges," *Sensors and Actuators, Part A*, Vol.33, pp.249, 1992.
- [23] L. Fan, R. Chen, A. Nespola and M. Wu, "Universal MEMS Platforms for Passive RF Components: Suspended Inductors and Variable Capacitor," *MEMS'98*, 1998.
- [24] H. Wu, K. Harsh, R. Irwin, W. Zhang, A. Mickelson, Y. Lee and J. Dobsa, "MEMS Designed for Tunable Capacitors," *Digest of the 1998 IEEE MTT Intl. Microwave Symposium*, pp.127, 1998.
- [25] A. Dec and K. Suyama, "Micromachined Electro-Mechanically Tunable Capacitors and Their Application to RF ICs," *IEEE Trans. Microwave Theory and Tech.*, Vol. 46, No.12, pp.2587, 1998.
- [26] J. Mink and D. Rutledge, "Guest Editor's Overview of the Special Issue on Quasi-Optical Techniques," *IEEE Trans. Microwave Theory Tech.*, pp.1661, Oct. 1993.
- [27] W. Lam, C. Jou, H. Chen, K. Stolt, N. Luhmann and D. Rutledge, "Millimeter-Wave Diode-Grid Phase-Shifters," *IEEE Trans. Microwave Theory Tech.*, pp.902, May 1988.
- [28] L. Sjogren, H. Liu, F. Wang, T. Liu, X. Qin, W. Wu, E. Chung, C. Domier and N. Luhmann, "A Monolithic Diode Array Millimeter-Wave Beam Transmittance Controller," *IEEE Trans. Microwave Theory Tech.*, pp.1782, Oct. 1993.
- [29] X. Qin, W. Zhang, C. Domier, N. Luhmann, W. Berk, S. Duncan and D. Tu, "Monolithic Millimeter-Wave Beam Control Array," *Digest of IEEE Microwave Theory Tech. Symposium*, pp.1669, 1995.
- [30] J.-C. Chiao and D. Rutledge, "Microswitch Beam-Steering Grid," *The Intl. Conference on Millimeter Submillimeter Waves Applications*, Jan. 1994.
- [31] J. Mazotta, M. DeLisio and J.-C. Chiao, "Quasi-Optical Discrete Beam Steering Grids," *IEEE MTT-S International Microwave Symposium*, June 1999.
- [32] J. Mazotta, L. Chen and J.-C. Chiao, "Reconfigurable Transmission-Type Beamformer," *IEEE MTT-S International Microwave Symposium*, June 2000.
- [33] B. Elamaram, I. Chio, L. Chen and J.-C. Chiao, "A Beam-Steerer Using Reconfigurable PBG Ground Plane," *IEEE MTT- S International Microwave Symposium*, June 2000.
- [34] F.-R. Yang, K.-P. Ma, Y. Qian and T. Itoh, "A Uniplanar Compact Photonic-Bandgap (UC-PBG) Structure and its Applications for Microwave Circuits," *IEEE Trans. Microwave Theory Tech.*, No. 8, pp. 1509-1514, 1998.